

We are IntechOpen, the world's leading publisher of Open Access books Built by scientists, for scientists

6,900

Open access books available

186,000

International authors and editors

200M

Downloads

Our authors are among the

154

Countries delivered to

TOP 1%

most cited scientists

12.2%

Contributors from top 500 universities



WEB OF SCIENCE™

Selection of our books indexed in the Book Citation Index
in Web of Science™ Core Collection (BKCI)

Interested in publishing with us?
Contact book.department@intechopen.com

Numbers displayed above are based on latest data collected.
For more information visit www.intechopen.com



Preparation and Properties of BaTiO₃ and Ba(Zr,Ti)O₃ Ceramics by Spark Plasma Sintering

Hiroshi Maiwa
Shonan Institute of Technology
Japan

1. Introduction

In this chapter, the dielectric and electromechanical properties of Ba(Zr_{0.2}Ti_{0.8})O₃ and BaTiO₃ ceramics prepared by spark plasma sintering (SPS) are reported. Those of ceramics prepared by conventional sintering are also reported for comparison with the SPS-prepared ceramics. The obtained information is helpful for possible application to the fabrication of lead-free piezoelectrics.

1.1 BaTiO₃ and Ba(Zr,Ti)O₃

Barium titanate has recently attracted attention due to the demand for lead-free piezoelectrics. Barium titanate ceramics prepared by microwave sintering (Takahashi et al., 2006, 2008) or two-step sintering (Karaki et al., 2007) with fine grains approximately 1 μm in size show excellent piezoelectric properties. These high piezoelectric properties are considered to be due to the small grain size. It is well known that the suppression of grain growth results in low-density samples by conventional sintering. Therefore, spark plasma sintering (SPS) was applied in the present study.

Zr-doped BaTiO₃ (BZT) ceramics are interesting materials that exhibit linear field-induced strain for actuator applications. We have previously reported the microstructure and the dielectric and electromechanical properties of these materials in thin film form (Maiwa et al., 2010); however, a characterization of the ceramic BZT with fine grains has not yet been carried out.

1.2 Spark plasma sintering

SPS is a process that uses electrical discharge between particles under pressure of several megapascals. SPS enables a compact powder to be sintered to a high density at a relatively low temperature and with a shorter sintering period. (Munir et al., 2006, 2011) In addition, SPS has an advantage over conventional sintering in that it suppresses exaggerated grain growth. Thus far, SPS has been applied to fabricate various piezoelectric ceramics, the reported results indicate that SPS is a powerful technique and opens the possibility of processing ceramics with controlled sub-micron grain sizes. (Hungria et al., 2009) Lead titanate (Kakegawa, 2004), NaNbO₃ (Wada et al., 2003), and Na_xK_{1-x}NbO₃ (Zhang, 2006) ceramics have been prepared by SPS. SPS has also applied to prepare BaTiO₃ ceramics and exhibited high dielectric constant of 10000; however, electromechanical properties has not been reported (Takeuchi et al., 1999).

2. Experimental

2.1 Sample preparation

The starting powder used were commercial $\text{Ba}(\text{Zr}_{0.1}\text{Ti}_{0.9})\text{O}_3$ and $\text{Ba}(\text{Zr}_{0.2}\text{Ti}_{0.8})\text{O}_3$ ceramic powder (Sakai Chemicals, Japan) and BaTiO_3 ceramic powder (Toda Kogyo, Japan). These powders were prepared by the hydrothermal method. The purities of the sample powder were more than 99%. In the case of conventional sintering, the powder was supplemented with 1% polyvinyl alcohol (PVA) binder, pressed in a die at a pressure of 80 MPa and sintered in air for 2 h from 1100 to 1450°C. In the case of SPS, no binder was added to avoid residual organics. Since the pellet is pressed during SPS, a binder is not required. For SPS, SPS-511S (SPS Syntex Inc., Japan) was used; raw powder was placed in a graphite die (10 mm diameter), and sintering was carried out in air atmosphere at a pressure of 60 MPa. The temperature was increased to 900-1100°C within 11 minutes and maintained at that temperature for 5 minutes, after which the pressure was released and the sample was cooled to room temperature. Since the pellet as-sintered by SPS at 1100°C is black and conductive, the pellet was annealed at 900-1400°C for 12 h in air.

2.2 Characterization

The surface of the sintered ceramics was observed by scanning electron microscopy (SEM, Hitachi S-2100A). The sintered samples were polished and then produced electrodes using a silver paste. Measurements of the electric field-induced displacement and polarization in BZT ceramics were performed using displacement sensor (Mahr GmbH, Millimar Nr. 1301, Germany) and a charge-amplifier circuit (Kitamoto Electronics, POEL-101, Japan). An alternating electric field of 0.1 Hz was used in these measurements. Prior to the small-signal measurements, including resonant-antiresonant methods and d_{33} measurements with the d_{33} meter, the ceramic specimens were polarized for 20 min in a silicone bath under a DC field of 20 kV/cm at room temperature. The resonant-antiresonant methods were carried out using an impedance analyzer (HP 4192A) for an additional 24 h after the polarization. The d_{33} meter (Chinese Academy of Science ZJ-3B, China) was used for the d_{33} measurements.

3. Structure and properties

3.1 $\text{Ba}(\text{Zr},\text{Ti})\text{O}_3$

Dielectric properties were evaluated in both $\text{Ba}(\text{Zr}_{0.1}\text{Ti}_{0.9})\text{O}_3$ and $\text{Ba}(\text{Zr}_{0.2}\text{Ti}_{0.8})\text{O}_3$ ceramic. Structure and electromechanical and piezoelectric properties were evaluated mainly in $\text{Ba}(\text{Zr}_{0.2}\text{Ti}_{0.8})\text{O}_3$ (BZT20) ceramic.

3.1.1 Density and microstructure

$\text{Ba}(\text{Zr}_x\text{Ti}_{1-x})\text{O}_3$ (BZT, $x=0.1$, and 0.2) ceramics are prepared by SPS and conventional sintering. By application of SPS, the $\text{Ba}(\text{Zr},\text{Ti})\text{O}_3$ ceramics with more than 96% relative densities could be obtained by the sintering at 1100°C for 5 minutes in air atmosphere. The grain growth is suppressed in the ceramics prepared by SPS, the average grain sizes were less than 1micron. Carbon contents of SPS prepared BZT ceramics and the conventionally sintered BZT are 0.15% and 0.024%, respectively. (Maiwa, 2008b) It should be noted that the SPS prepared BZT ceramics examined carbon content contained organic binder intentionally for comparison. Since the organic binder is not added to SPS prepared ceramics usually, carbon contents of the SPS prepared ceramics would be less than 0.15%.

The SPS-BZT20 ceramics prepared by SPS at 1100°C and then annealed at 1100°C, 1200°C, and 1300°C were 5.89, 5.87, and 5.83 g/cm³, respectively. These ceramics were almost fully sintered. SEM images of the BZT20 ceramics prepared by SPS and normal sintered are shown in Figs. 1 and 2, respectively. The SPS-BZT20 ceramics annealed at 1200°C were found to have very small grains less than 1 μm in diameter. In the SPS-BZT20 ceramics annealed at 1300°C, small grains less than 1 μm in diameter and relatively large grains several tens of microns in diameter coexisted. Since SPS provided rapid sintering at 1100°C within 5 minutes, grain growth was suppressed. As described later, grain growth is limited by normal sintering at 1300°C and lower, and the fine grains of as-SPS ceramics are taken over after a lower post-annealing temperature of 1200 and 1300°C. The grains of the SPS-BZT20 ceramics annealed at 1400°C were all relatively large, more than several tens of microns in diameter.

In conventional sintering, the relative density was found to increase and the grains grew with increases in the sintering temperature. The relative densities of the ceramics sintered at 1300, 1350, 1400, and 1450°C were 4.67, 5.03, 5.68, and 5.77 g/cm³, respectively. These values were lower than those of the SPS-BZT20 ceramics. It should be noted that the normally sintered ceramics contained pores, as show in Fig. 2. The average grain sizes were approximately 1 μm for the samples annealed at 1300-1400°C, with the size increasing slightly with temperature. Grain growth occurred over the range from 1400-1450°C.

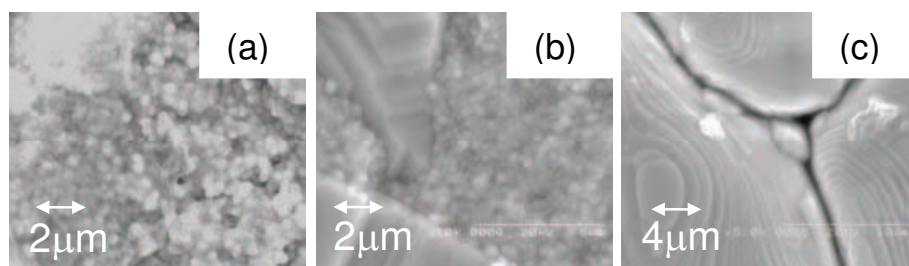


Fig. 1. SEM images of the Ba(Zr_{0.2}Ti_{0.8})O₃ ceramics SPS-prepared at 1000°C and annealed at (a) 1200, (b) 1300°C, and (d) 1400 °C.

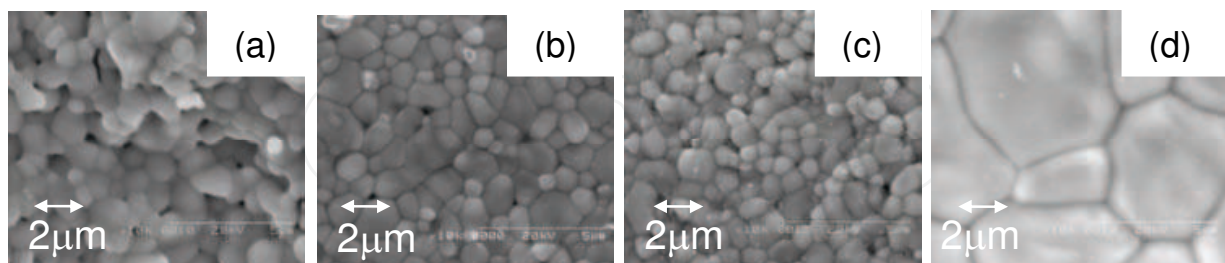


Fig. 2. SEM images of the Ba(Zr_{0.2}Ti_{0.8})O₃ ceramics normally sintered at (a) 1300, (b) 1350, (c) 1400, and (d) 1450.

3.1.2 Dielectric properties

Figure 3 and 4 show the temperature dependence of the dielectric constant and loss tangent of the Ba(Zr_{0.1}Ti_{0.9})O₃ and Ba(Zr_{0.2}Ti_{0.8})O₃ ceramics in the temperature range of 30 - 150°C, respectively. The dielectric anomalies in these Ba(Zr_{0.1}Ti_{0.9})O₃ and Ba(Zr_{0.2}Ti_{0.8})O₃ ceramics occur at approximately 90 and 40°C, respectively. These coincide well with reported values.

With increasing sintering temperature in normal sintering, the jumps accompanying the dielectric anomaly become clear. The temperature dependence of the SPS-prepared BZT ceramics is relatively mild, and the nominal value is higher than that of the sample sintered at relatively lower temperatures of 1200 and 1250°C. The mild temperature dependence of the SPS BZT ceramics is considered to be due to small grains. The relatively high dielectric constant is attributed to the high density.

It was reported that by Takeuchi et al. BaTiO₃ SPS-prepared at 1000°C and with grains less than 1 μm does not show a broadening transition but a sharp transition. (Takeuchi et al, 1999) Kinoshita et al. reported that fine-grained BaTiO₃ ceramics with 1.1 μm grains exhibit sharp transition. (Kinoshita & Yamaji 1976) In this study, the broad transitions are observed in Ba(Zr_{0.1}Ti_{0.9})O₃ ceramics with 0.56 μm grains and Ba(Zr_{0.2}Ti_{0.8})O₃ ceramics with 0.86 μm and 0.53 μm grains. At present, the reason for the difference in transition between pure BaTiO₃ and zirconium-containing BaTiO₃ system is not clear. It is considered that the relaxor nature of the zirconium-containing BaTiO₃ system induces a broadening of the transition in ceramics with larger grains, than pure BaTiO₃ ceramics. In the BaTiO₃-BaZrO₃ system, dielectric relaxation is induced by the addition of nonpolar BaZrO₃, and disorder is considered to be expanded by separating a large number of small grains. The transition is further broadened in small-grained samples of SPS Ba(Zr_{0.2}Ti_{0.8})O₃, supporting the above speculations.

There is another point to be compared with pure BaTiO₃. It has been reported that the dielectric constant of pure BaTiO₃ at room temperature has been determined for ceramics of approximately 1 μm grain size. In this study, no marked increase in dielectric constant at room temperature is observed in Ba(Zr_{0.1}Ti_{0.9})O₃ and Ba(Zr_{0.2}Ti_{0.8})O₃ ceramics. Compared with the conventionally sintered ceramics of the same grain size, the SPS-prepared Ba(Zr_{0.1}Ti_{0.9})O₃ and Ba(Zr_{0.2}Ti_{0.8})O₃ ceramics exhibit relatively larger dielectric constants at room temperature; however, this is mainly due to the increase in their densities.

The dielectric properties of the SPS-prepared ceramics are understood to be dependent on the enlargement of the small grains of the ceramics sintered at low temperature, as shown in Fig. 1. It is reasonable to say that no marked increase in the dielectric properties of the materials occurs in the SPS-prepared samples; however, the elimination of pores plays a major role in increasing dielectric constant. It is difficult to discuss the effect of density on dielectric constant quantitatively. Conductivity affects dielectric constant through capacitance; however, is difficult to take conductance into account in the calculation of dielectric constant. Moreover, the formularization of pore distribution is difficult. By assuming a model of a series of capacitors consisting of air and dielectrics materials, the thicknesses ratio of air to the dielectrics of 1/1000, and a dielectric constant of 5000 in the dielectrics, the measured dielectric constant becomes 17% of the pure dielectrics. Although this model is too simple; however, it shows that the elimination of pores enhances the dielectric constant, and it can roughly explain the high dielectric constant of the dense ceramics prepared by SPS in the entire throughout measured temperature range. In other words, the dielectric constants of the small-grained Ba(Zr_{0.1}Ti_{0.9})O₃ and Ba(Zr_{0.2}Ti_{0.8})O₃ ceramics are weakly temperature-dependent basically. The low dielectric constants of the small-grained ceramics normally sintered are due to the low density. While, SPS-prepared ceramics are dense and composed of small grains, their dielectric constant is high and weakly temperature-dependent.

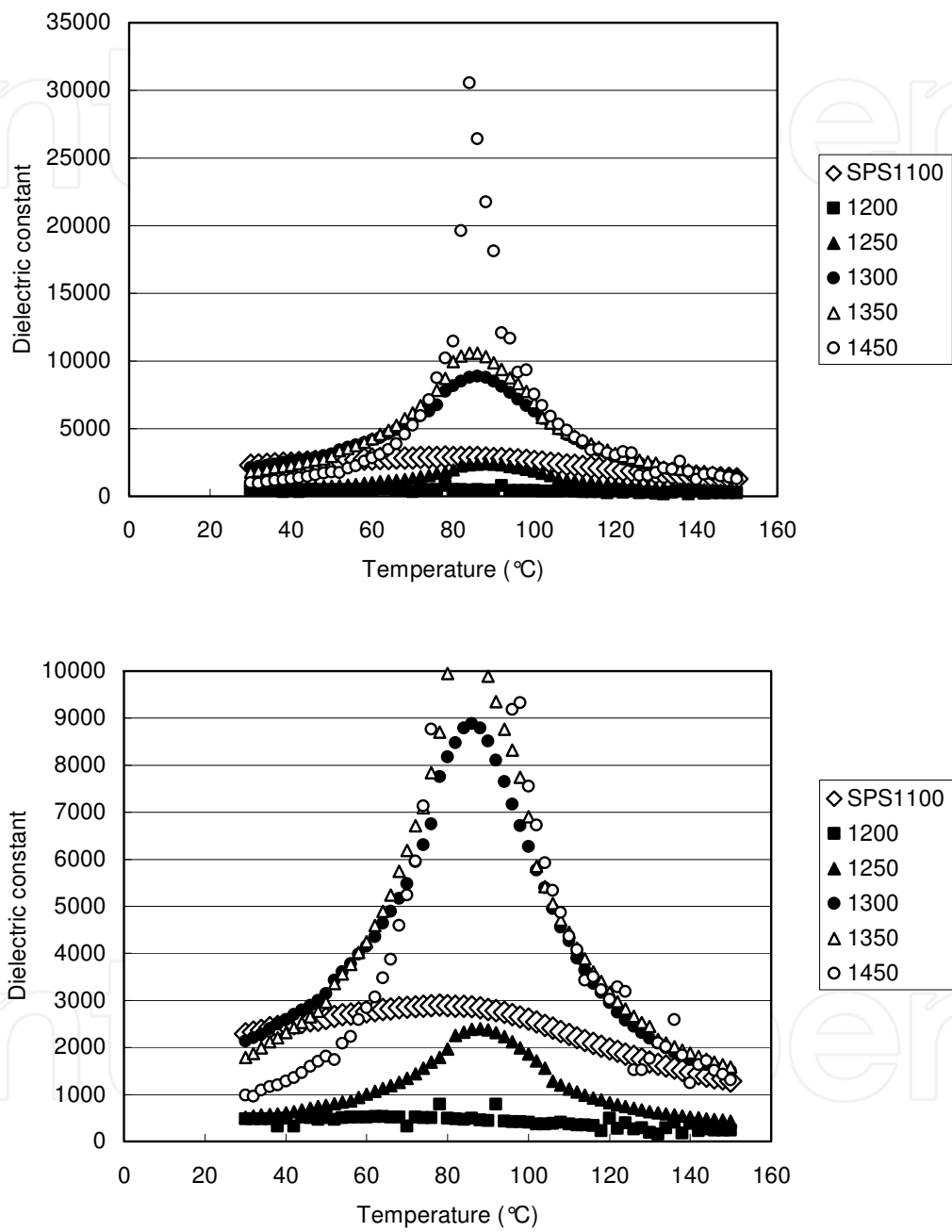


Fig. 3. Temperature dependences of (a) dielectric constant, (b) dielectric constant (expanded), of Ba(Zr_{0.1}Ti_{0.9})O₃ ceramics.

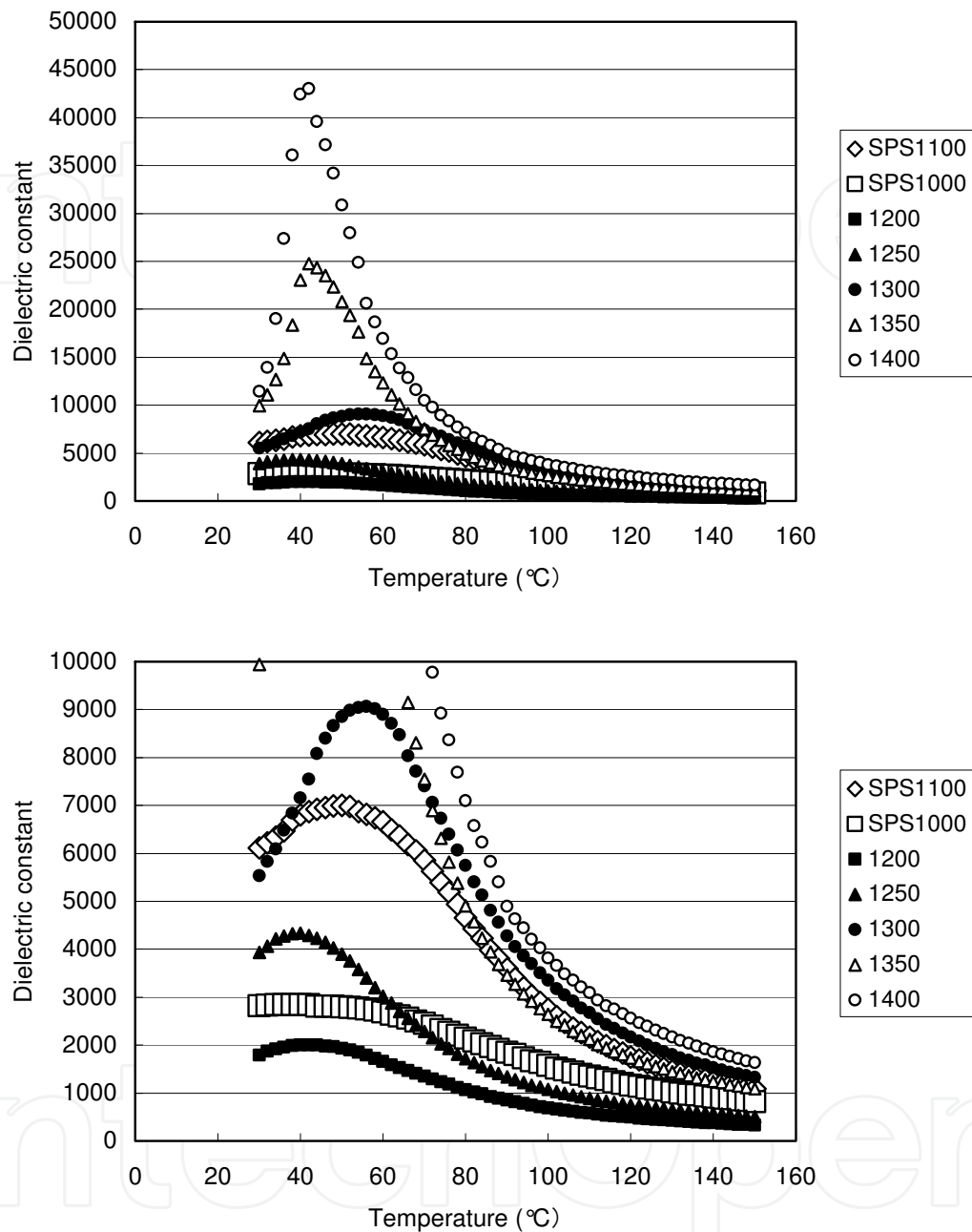


Fig. 4. Temperature dependence of (a) dielectric constant, (b) dielectric constant (expanded), of $\text{Ba}(\text{Zr}_{0.2}\text{Ti}_{0.8})\text{O}_3$ ceramics.

The ceramics with low density exhibit a relatively high loss tangent, probably due to a large numbers of defects. SPS and normally sintered ceramics with high densities exhibit smaller loss tangent, generally less than 2%. An increase in loss tangent accompanying dielectric anomaly is more clearly seen in the $\text{Ba}(\text{Zr}_{0.2}\text{Ti}_{0.8})\text{O}_3$ ceramics, probably due to the greater diffusivity of the transition.

3.1.3 Electromechanical properties

The Strain/Field in the SPS Ba(Zr_{0.1}Ti_{0.9})O₃ and Ba(Zr_{0.2}Ti_{0.8})O₃ are 76pm/V under 24.5kV/cm and 252pm/V under 13.9kV/cm, respectively. Figures 5 and 6 show the field-induced strain of SPS-BZT20 ceramics annealed at 1200 and 1300°C and the BZT20 ceramics normally sintered at 1300 - 1450 °C, respectively. The SPS-BZT20 ceramics annealed at 1200°C exhibited a strain loop with less shrinkage and lower displacement. Since the strain hysteresis behavior accompanying shrinkage is derived from ferroelectric domain switching, ferroelectric domain activities are suppressed, probably due to the residual stress or small grains, or both. The SPS-BZT20 annealed at 1300°C exhibited a strain loop with large shrinkage and larger displacement. The SPS-BZT annealed at 1400°C was too leaky to measure the dynamic strain loop under application of a DC field of 10kV/cm and higher.

In the case of normal sintering, the BZT20 ceramics sintered at 1350°C exhibited the highest strain among the samples measured. The sample sintered at 1300°C exhibited smaller strain due to the small grains, low density, or both. The samples sintered at 1400 and 1450°C exhibited smaller displacement than that sintered at 1350°C. The grain sizes of these samples were considered to be larger than appropriate for this material. The strain loops became more hysteretic with increasing sintering temperature. In the case of pure BaTiO₃, the ceramics with a grain size of 0.61-0.74 μm exhibited the largest field-induced strain, and the ceramics with smaller and larger grains exhibited lower strain. The results obtained here for BZT followed the grain size dependencies seen in pure BaTiO₃.

The unipolar field-induced strains of these samples were also measured. The general tendencies were the same as those observed with the bipolar strain loops. The dynamic strain/field at 20 kV/cm of SPS-BZT annealed at 1300°C and the BZT20 ceramics normally sintered at 1350 °C were 290 and 280 pm/V, respectively. These two values are comparable; however, the SPS-BZT20 yielded a more linear strain curve compared with the sample normally sintered at 1350°C. This difference can be shown clearly in the dependence of electric field on dynamic d₃₃, which is calculated from the strain/field. The results are shown in Fig. 7. Considering the relatively low dielectric constant of 1204, the reason for the linear strain of SPS-BZT20 is considered to be due to the suppressed polarization rotation. (Maiwa 2008a) The lower hysteretic strain with good linearity for the SPS-BZT20 ceramics is unique and might be desirable for actuator applications that require analogue operations.

3.1.4 Static piezoelectric properties

The clear resonances were observed only for the SPS-BZT annealed at 1300°C and the BZT20 ceramics normally sintered at 1400 °C, as shown in Fig. 6. The piezoelectric properties calculated by the resonance method are included in Table 1. In the case of the SPS-BT, the Q_m and k_p values are 44-62 and 16.2-17.5, respectively, which are smaller than the Q_m and k_p values of 325 and 25.1 (%) for the SPS-BZT20 annealed at 1300°C. The reason for this difference is not clear, but the unique microstructure composed of submicron and coarse grains might play a role in producing the reasonably high Q_m and k_p values. These ceramics exhibit a small loss tangent, generally less than 2%.

The d₃₃ values measured with the d₃₃ meter are shown in Fig. 7. This measurement method is more sensitive than dynamic measurement. The low values are derived from the insufficient polarization due to the grains being too small or high conductivity of the samples. The d₃₃ values for the SPS-BZT20 annealed 1300°C and the BZT20 ceramics

normally sintered at 1400 °C are of 126 and 138pC/N, respectively. Yu et al. have reported d_{33} values of 130pC/N measured in $\text{Ba}(\text{Zr}_{0.08}\text{Ti}_{0.92})\text{O}_3$ ceramics by resonance-antiresonance measurements (Yu et al., 2002), and the values obtained in this study are reasonable in comparison with the values.

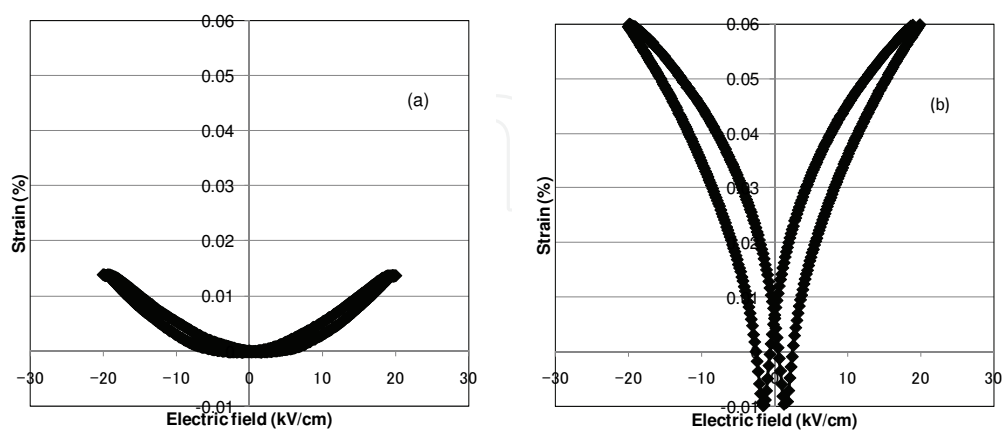


Fig. 5. Field-induced strain of the $\text{Ba}(\text{Zr}_{0.2}\text{Ti}_{0.8})\text{O}_3$ ceramics SPS-prepared at 1100°C and then annealed at (a)1200 and (b)1300°C.

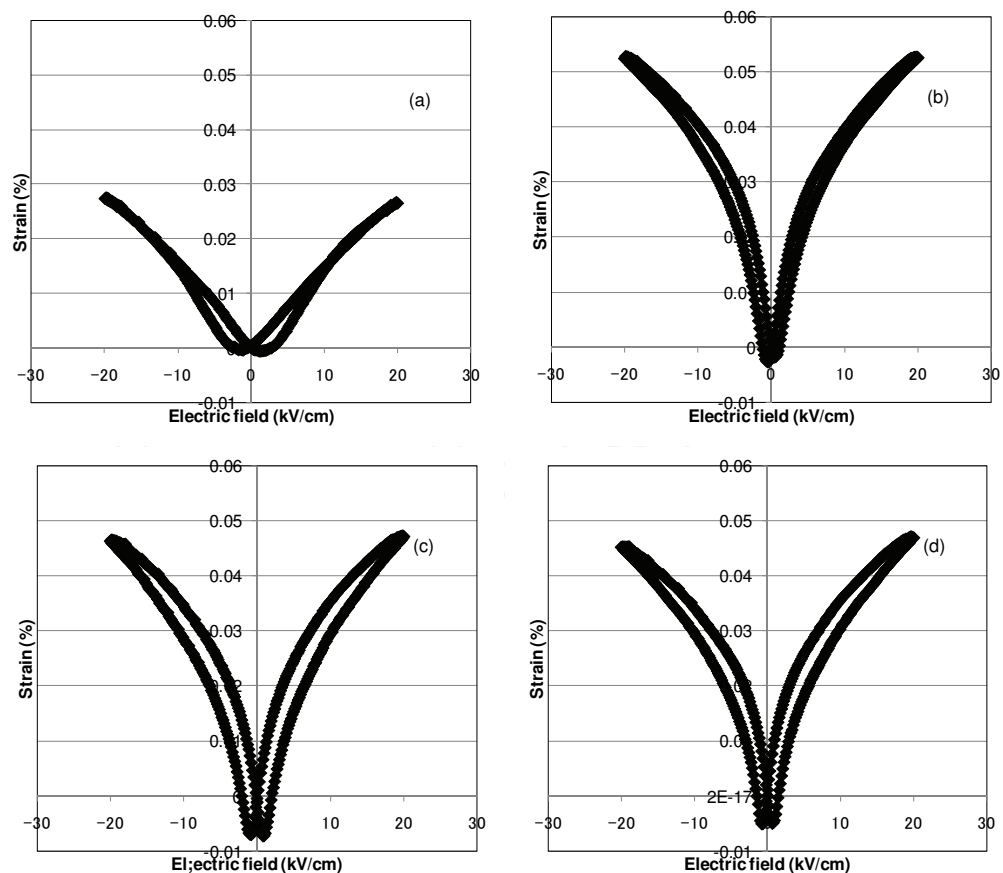


Fig. 6. Field-induced strain of the $\text{Ba}(\text{Zr}_{0.2}\text{Ti}_{0.8})\text{O}_3$ ceramics normally sintered at (a)1300, (b)1350, (c)1400, and (d)1450 °C.

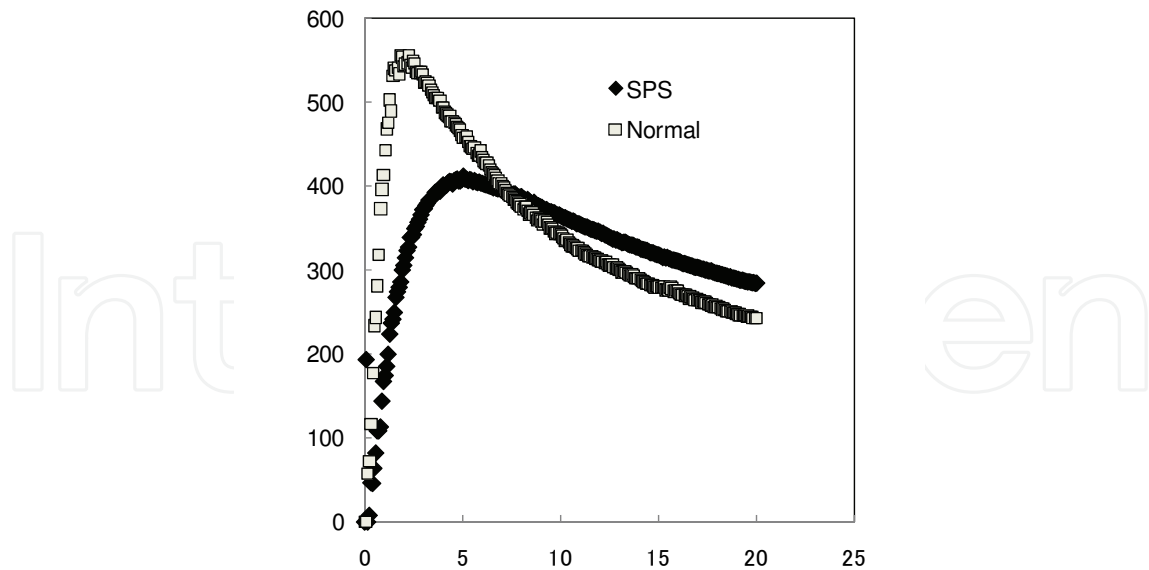


Fig. 7. Field dependence of the dynamic d_{33} calculated from the unipolar field-induced strain of the Ba(Zr_{0.2}Ti_{0.8})O₃ ceramics SPS-prepared at 1100°C (SPS) and then annealed at 1300°C and normally sintered at 1400°C (Normal).

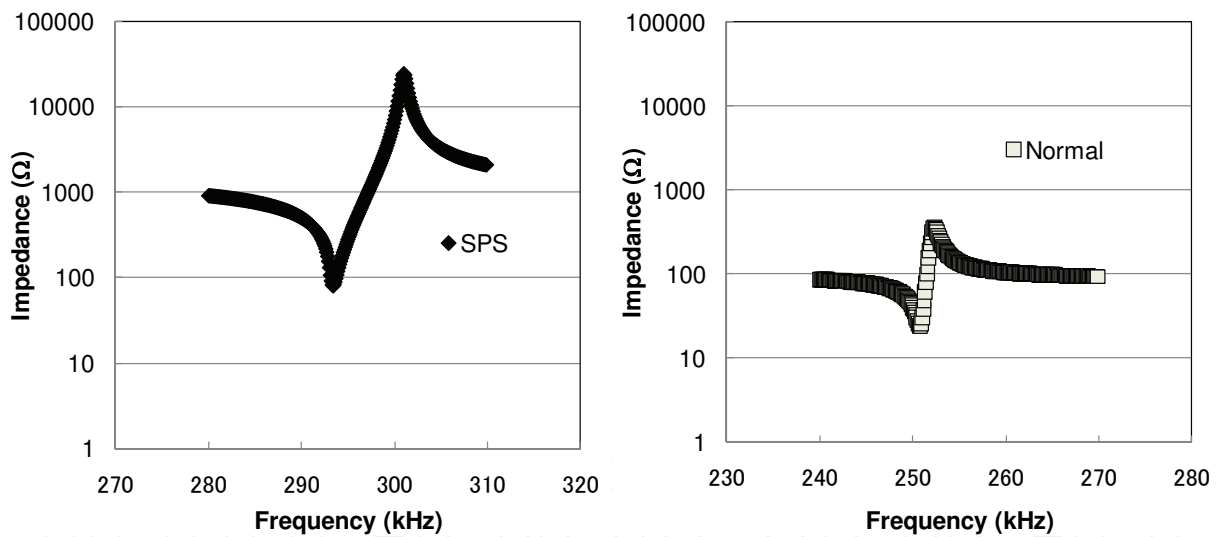


Fig. 8. Resonance-antiresonance measurement of the Ba(Zr_{0.2}Ti_{0.8})O₃ ceramics SPS-prepared at 1100°C and then annealed at 1300°C (SPS) and normally sintered at 1400°C (Normal).

Sample	Q _m	k _p (%)	Dielectric constant	d ₃₁ (10 ⁻¹² C/N)
SPS1300	312	25	1204	43
Normal 1400	119	21	7869	91

Table 1. Piezoelectric properties of the Ba(Zr_{0.2}Ti_{0.8})O₃ ceramics SPS-prepared at 1100°C and then annealed at 1300°C (SPS1300) and normally sintered at 1400°C (Normal 1400).

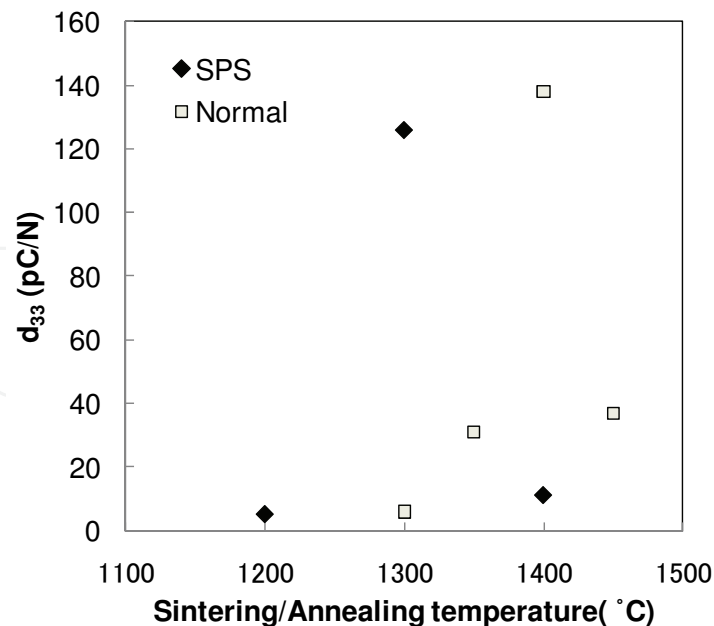


Fig. 9. The d_{33} values measured by d_{33} meter.

3.2 BaTiO₃

Density, dielectric and preliminary electromechanical properties were evaluated in the BaTiO₃ ceramics SPS-prepared at 900°C. Electromechanical and piezoelectric properties were evaluated mainly in the BaTiO₃ ceramics SPS-prepared at 950°C.

3.2.1 Density and microstructure

The as-sintered pellet prepared by SPS at 900-1100 °C was black and conductive. Although SPS was carried out in air atmosphere, the samples were deoxidized by heating the carbon die. By post-annealing at 900-1200 °C for 12 h in air, the pellet was oxidized and became white and insulating. These features are similar to those of the Ba(Zr,Ti)O₃. The relative densities of the BT ceramics prepared by SPS at 900-1100 °C were 5.84-5.97 g/cm³. These ceramics are almost fully sintered. Compared with Ba(Zr_{0.2}Ti_{0.8})O₃ ceramics, the BT ceramics can be sintered at lower temperatures. This is due to the smaller particle size or the nature of the pure BT. In conventional sintering, the relative densities of the samples increase with sintering temperature, as shown in Fig. 10. SEM images of the BT ceramics prepared by conventional sintering and by SPS are shown in Figs. 11 and 12, respectively. The average grain sizes of samples of these ceramics are shown in Fig. 13. It is noted that grain growth is promoted by high-temperature annealing and suppressed by SPS. The average grain sizes of the BT ceramics prepared by SPS at 900-1200 °C, which increase with annealing temperature, are below 1 μm. These values are almost equivalent to those of ceramics of the same composition conventionally sintered at 1100-1200 °C. Figures 14 and 15 show the X-ray diffraction patterns of the BT ceramics prepared by normal sintering and by SPS, respectively. The diffraction peaks of the starting powder are broad and no splits due to the distortion from cubic structure are observed. The cubic structure of fine BT powder has been frequently reported. The peaks of the as-SPS ceramics, the ceramics prepared by SPS without annealing, are broad and shifted to a lower angle. The lattice elongation is caused by deoxidization. The X-ray diffraction patterns of the ceramics conventionally sintered at

1100 °C and the ceramics prepared by SPS at 900 °C and then annealed at 900-1100 °C were different in terms of the normal splitting peaks, with 1:2 intensity ratio of tetragonal (002) and (200) observed in the ceramics conventionally sintered at 1200 and 1300 °C. This is due to the structural change derived from the stress in the small grain below 1 μm.

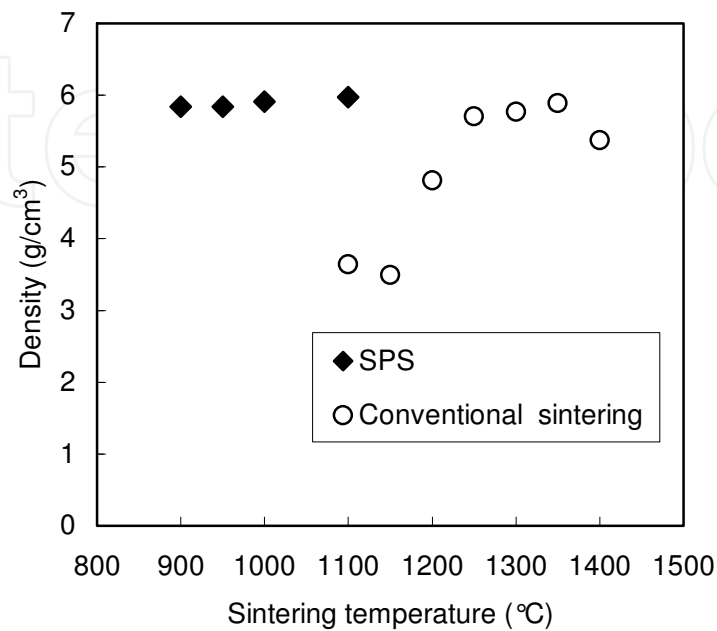


Fig. 10. Relative densities of BaTiO₃ samples.

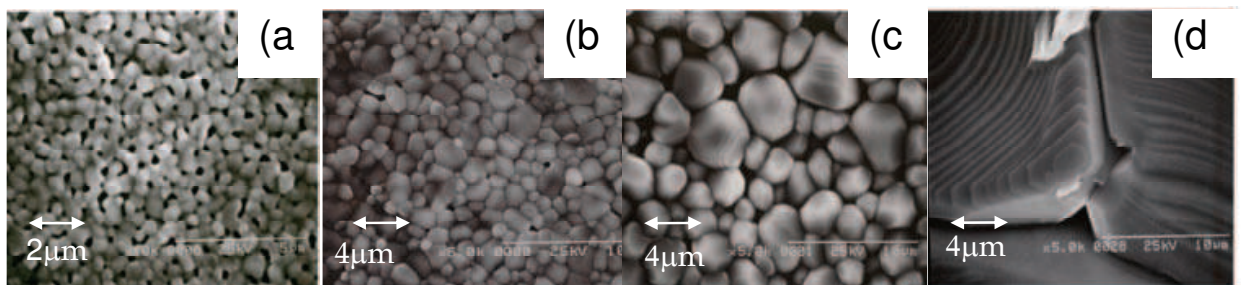


Fig. 11. SEM images of the BaTiO₃ ceramics normally sintered at (a) 1100, (b) 1200, (c) 1300, and (d) 1400 °C.

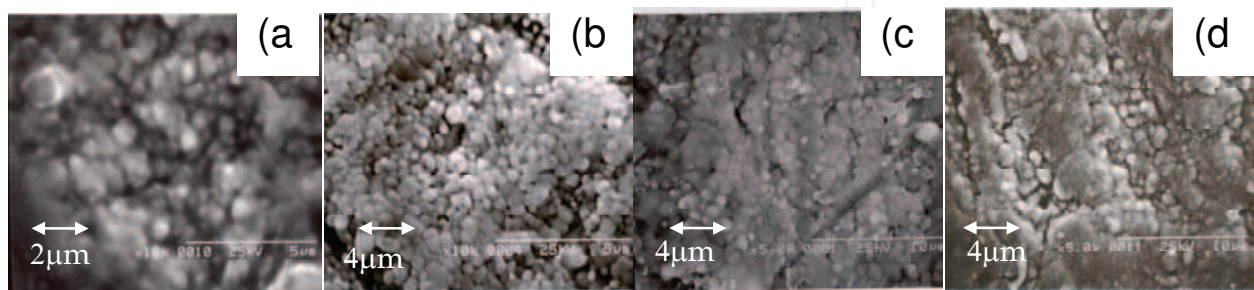


Fig. 12. SEM images of the BaTiO₃ ceramics SPS-prepared at 900 °C and then sintered at (a) 900, (b) 1000, (c) 1100, and (d) 1200 °C.

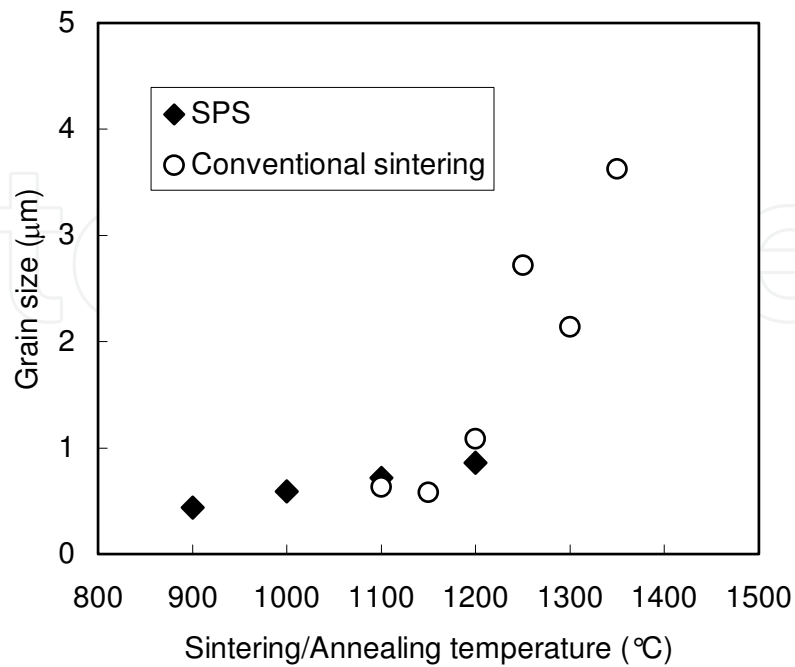


Fig. 13. Average grain sizes of BaTiO₃ samples.

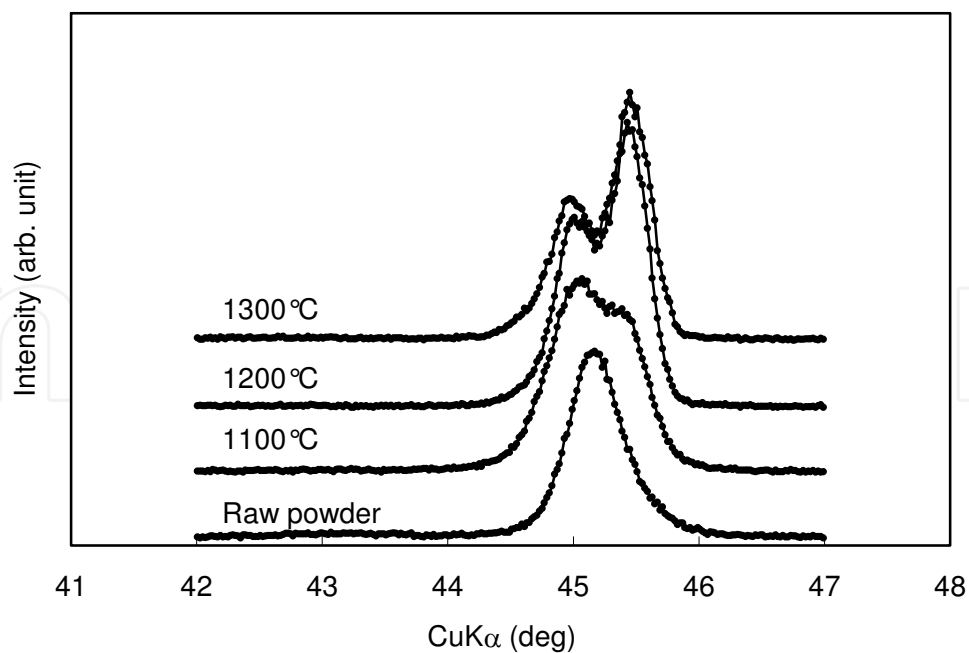


Fig. 14. X-ray diffraction patterns of starting powder and the BaTiO₃ ceramics conventionally sintered at 1100, 1200, and 1300 °C.

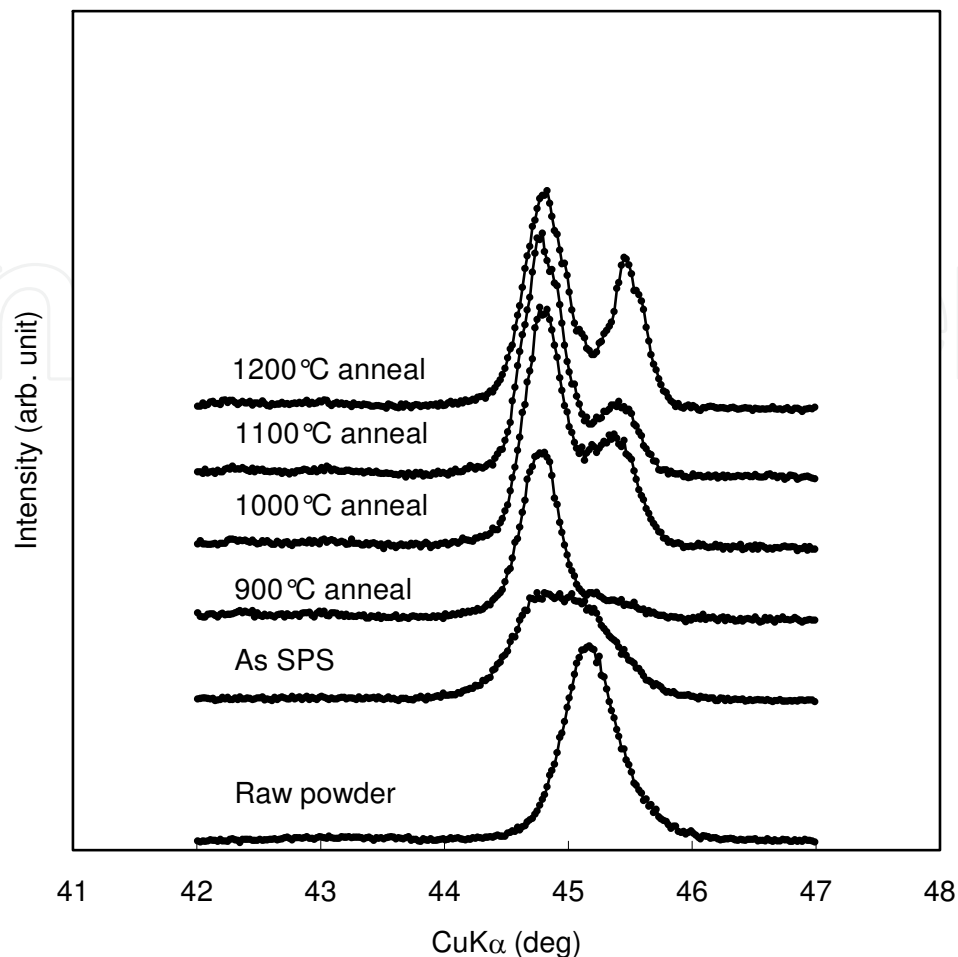


Fig. 15. X-ray diffraction patterns of starting powder and the BaTiO₃ ceramics SPS-prepared at 900°C and then sintered at (a) 900, (b)1000, (c) 1100 and (d)1200 °C.

3.2.2 Dielectric properties

Figure 16 shows the dielectric constant of the BT ceramics at room temperature. Figure 17 shows the temperature dependence of the dielectric constant of the BT ceramics prepared by normal sintering and by SPS in the temperature range of 30-150 °C. The dielectric constants at room temperature of the BT ceramics prepared by SPS and then annealed at 1000 and 1100 °C, whose grains are 0.61-0.74 μm in size, are highest among the samples prepared in this study. This result agrees well with the reported values. It was reported by Takeuchi et al. that BT ceramics SPS-prepared at 1000 °C with grains of less than 1 μm size, showed a dielectric constant of 10000. (Takeuchi et al., 1999) Kinoshita and Yamaji reported that the fine-grained BT ceramics with 1.1 μm grains exhibited a high dielectric constant of approximately 5000. (Kinoshita & Yamaji, 1976) Arlt et al. reported that the fine-grained BT ceramics with 0.7 μm grains exhibited a high dielectric constant of approximately 5000 at room temperature. (Arlt et al., 1985)

The transition temperature is another point to be compared with previous reports on pure BT. The dielectric anomalies in the BT ceramics occur at approximately 120 °C. In this study, a lowering dielectric anomaly with annealing temperature was observed, as shown in Fig. 17. Kinoshita and Yamaji reported that the fine-grained BaTiO₃ ceramics with 1.1 μm grains

exhibited a negligible shift compared with the ceramics with 53 μm grains. (Kinoshita & Yamaji, 1976) Takeuchi et al. reported that the BT ceramics SPS-prepared at 1000 $^{\circ}\text{C}$ and with grains of less than 1 μm size showed a shift in the Curie temperature. (Takeuchi et al., 1999) It has been reported that the Curie temperature of the pure BT ceramics with fine grains shifts to a lower temperature. (Line & Glass, 1977) (Xu et al., 1989) The decrease in the Curie temperature is due to the effects of the fine grains.

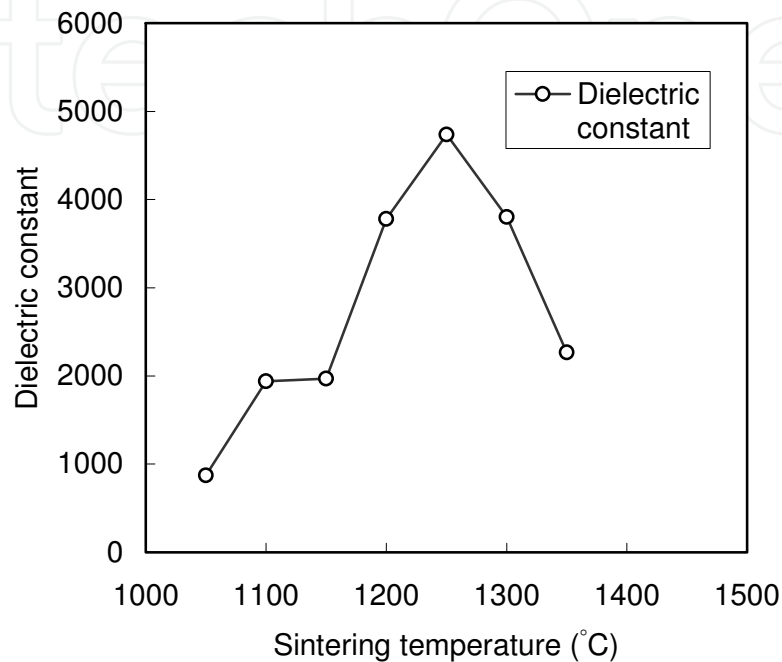


Fig. 16. Dielectric constant of the conventionally sintered BaTiO_3 ceramics.

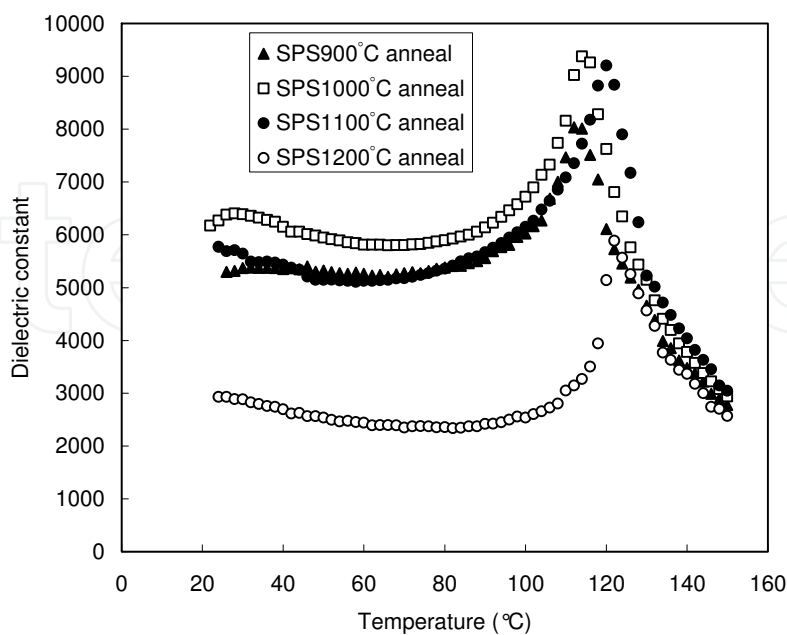


Fig. 17. Temperature dependence of dielectric constant of the BaTiO_3 ceramics SPS-prepared at 900 $^{\circ}\text{C}$ and then sintered at (a) 900, (b)1000, (c) 1100 and (d)1200 $^{\circ}\text{C}$.

3.2.3 Electroimechanical properties

The field-induced displacement of the BT ceramics prepared by SPS at 900 °C were measured. The bipolar field-induced strain loops of the BT ceramics prepared by SPS and then annealed at 900-1200 °C are shown in Fig. 18. With increasing annealing temperature, the strain loops became slim. This is due to the ease of the domain motion in larger grains. A larger displacement of the BT ceramics prepared by SPS was observed in the samples annealed at 1000 and 1100 °C, which have larger dielectric constants than the samples annealed at 900 and 1200 °C. The unipolar field-induced strain loops and calculated dynamic d_{33} of the BT ceramics prepared by SPS and then annealed at 1000 and 1100 °C are measured. (Maiwa 2008a) The strain/field values at 15 kV/cm of the BT ceramics prepared by SPS and then annealed at 1000 and 1100 °C are 540 and 530 pm/V, respectively. These values are comparable to the reported high remanent d_{33} values of the BaTiO₃ ceramics prepared by microwave sintering or two-step sintering.

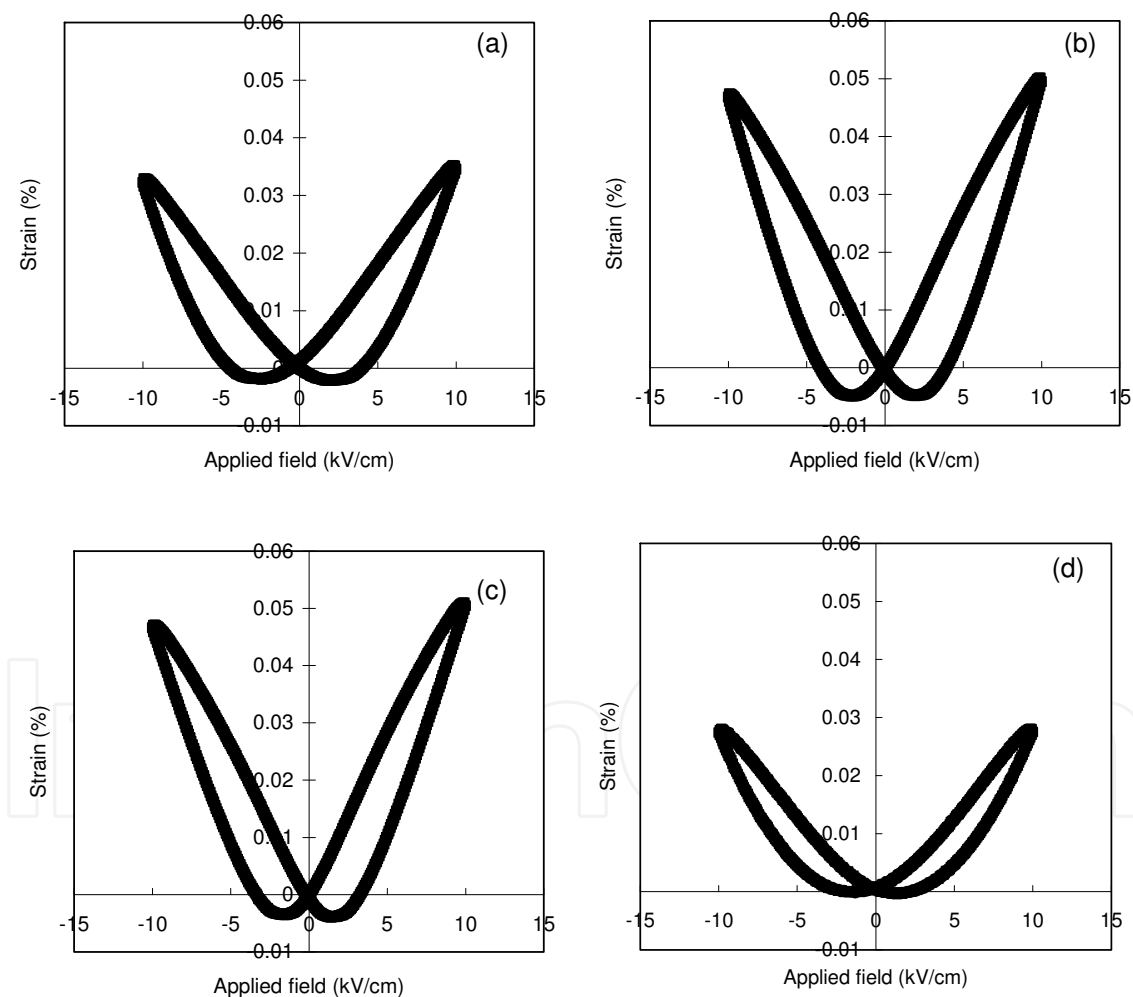


Fig. 18. Field-induced displacement of the BaTiO₃ ceramics SPS-prepared at 900 °C and then sintered at (a) 900, (b) 1000, (c) 1100 and (d) 1200 °C.

The bipolar polarization and field-induced strain loops of the SPS-BT, conventionally sintered, and two-step-sintered BT ceramics are shown in Figs. 19-21, respectively. Note that the SPS-BT ceramics exhibit relatively thin polarization loops. Large hysteretic strain loops

are obtained in the ceramics sintered at a high temperature of 1400 °C. The large hysteresis is due to the effects of polarization rotation in larger grains. The unipolar strain and derived dynamic d_{33} values of these BT ceramics are measured. (Maiwa, 2009) SPS-BT ceramics exhibit relatively large strains regardless of their fine grains. Compared with the fine-grained BT ceramics fabricated by other methods, such as the BT ceramics conventionally sintered at 1300 °C and the BT ceramics two-step-sintered at 1300 °C, the SPS-BT ceramics exhibit high d_{31} . The field-induced strain loops of the SPS-BT ceramics are linear; this corresponds to the flat dynamic d_{33} behavior under high field. Large hysteretic strain loops and high calculated d_{33} values are observed in the ceramics sintered at high temperature. The calculated d_{33} values of these samples decrease markedly under high field. These phenomena can be explained as follows. The samples exhibit large induced strains due to polarization rotation under low field, and the induced strains decrease together with the completion of polarization rotation. In the case of the SPS-BT ceramics, the observed linear strain behavior is considered to be due to the suppressed polarization rotation and electrostrictive strain reflected by the high dielectric constant, or both mechanisms.

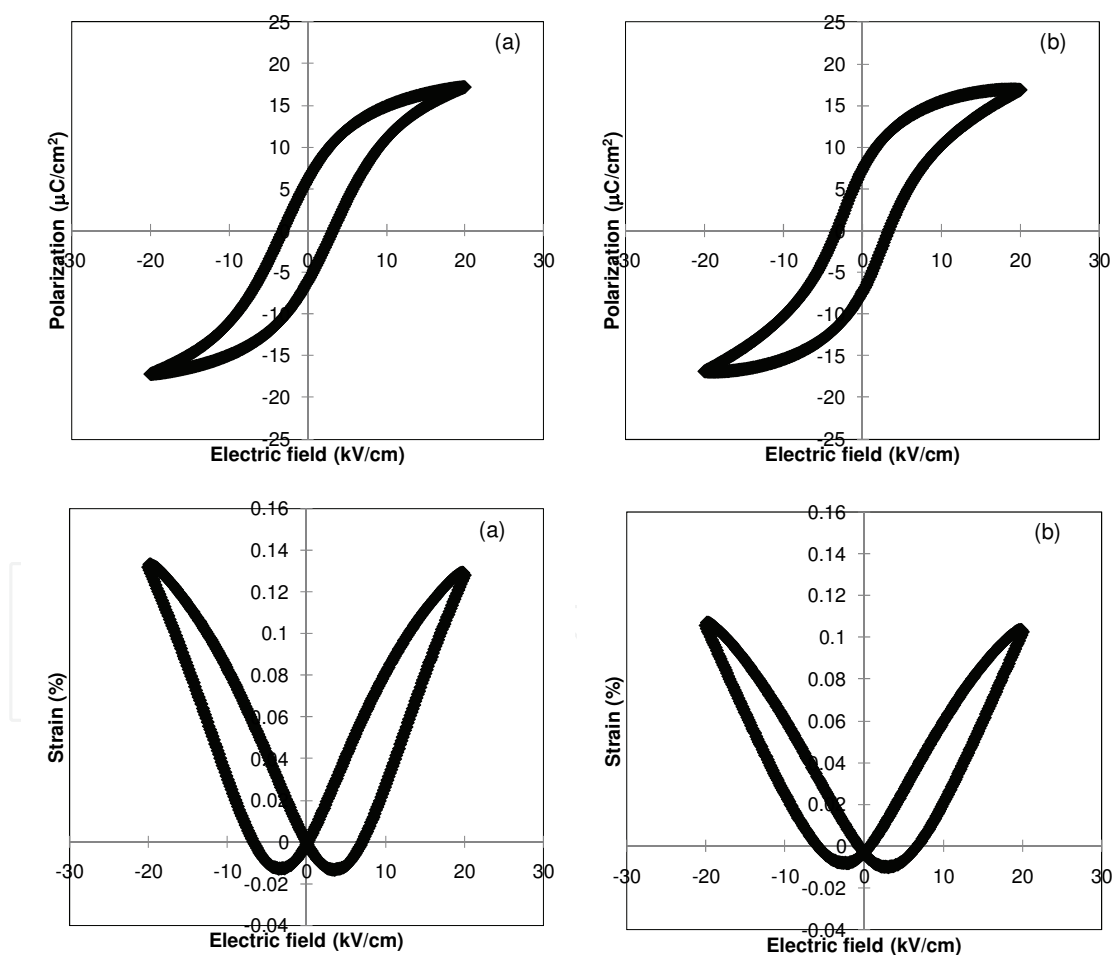


Fig. 19. Polarizations and field-induced strains of the BT ceramics SPS-prepared at 950 °C and then annealed at (a) 1000 and (b) 1200 °C.

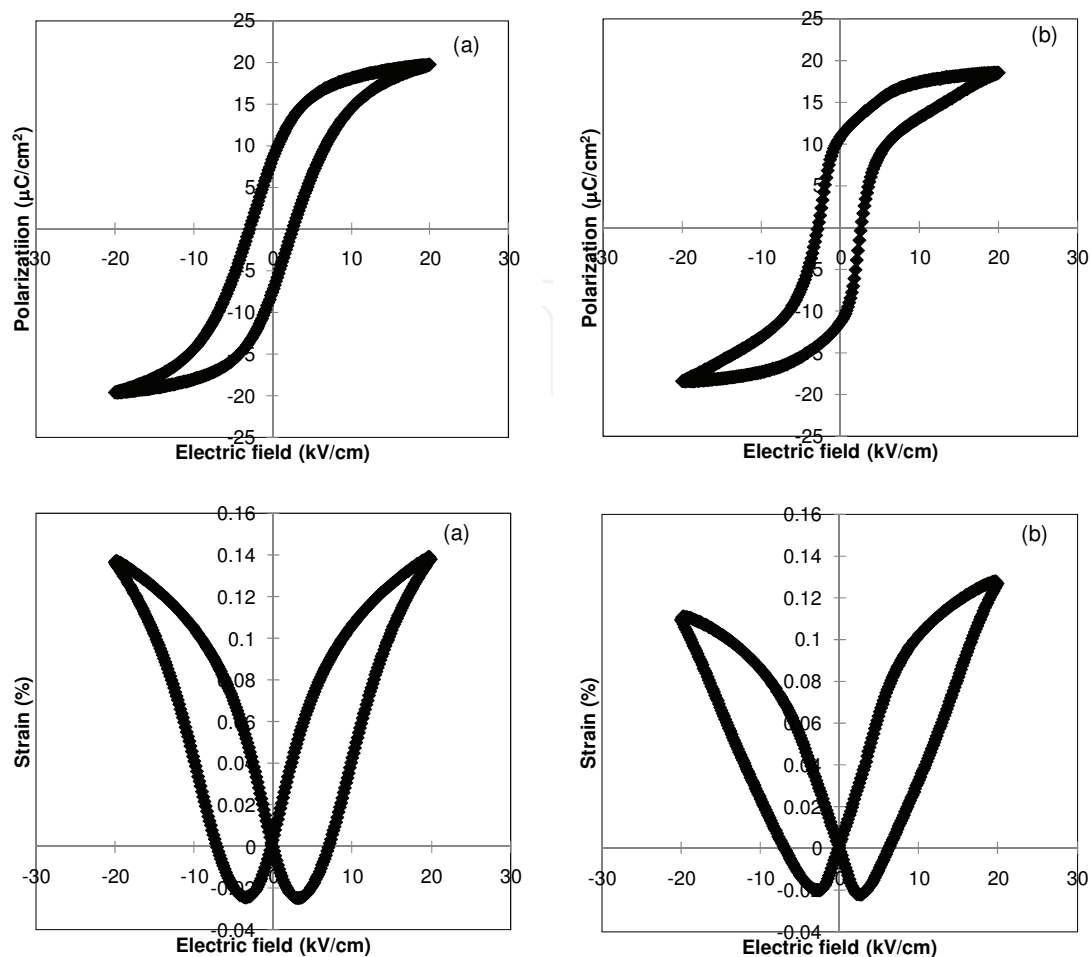


Fig. 20. Polarizations and field-induced strains of the BT ceramics conventionally sintered at (a) 1300 and (b) 1400 °C.

3.1.4 Static piezoelectric properties

The piezoelectric properties calculated by resonance methods are included in Table 2. The SPS-BT ceramics are characterized by high d_{31} and low Q_m . Compared with the fine-grained BT ceramics fabricated by other methods, the SPS-BT ceramics exhibit high d_{31} . Relatively high d_{31} values correspond to large field-induced strains. Here, I discuss the origin of the large difference between d_{31} obtained by the resonance methods and d_{33} calculated from the slope of the dynamic-field-induced strain measurement. The major differences of these measurements lie in the driving frequency and field amplitude. The frequencies and electric field amplitudes in the resonance methods and the dynamic measurement are 200-300 kHz and 14-15 V/cm, and 0.1 Hz and 20-30 kV/cm, respectively.

A slow and high-field dynamic measurement detects the displacement including polarization rotation that requires large energy. A rapid and low-field resonance method eliminates the displacement due to polarization rotation. The dynamic d_{33} values calculated from the linear part of the slope under a high field of more than 20 kV/cm are 200-350 pm/V generally. These values roughly correspond to twice the d_{31} value calculated by the resonance method, indicating that the explanations above are reasonable. Q_m is related to the internal stress. The low Q_m of the SPS-BT ceramics suggests the presence of high

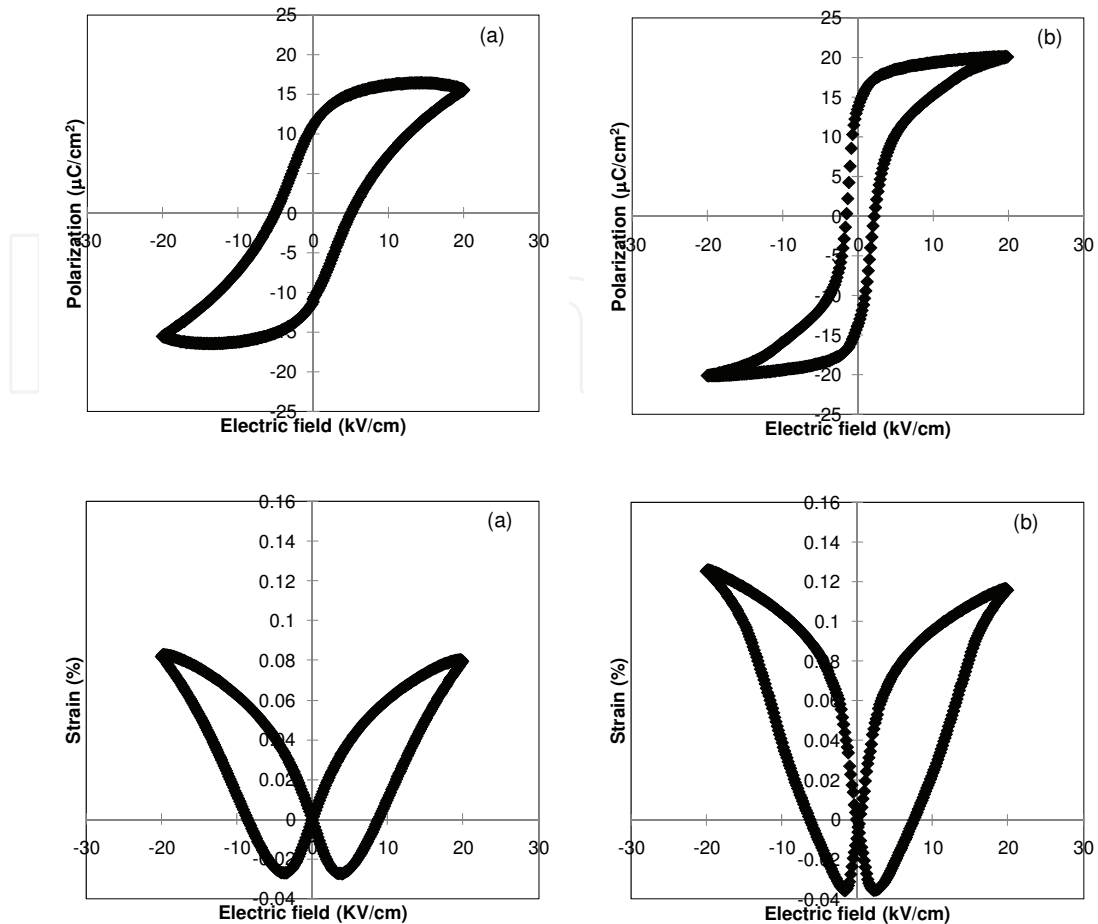


Fig. 21. Polarizations and field-induced strains of the BT ceramics two-step-sintered at (a) 1300 and (b) 1400 °C.

Sample	Density (g/cm ³)	Grain size (μm)	Qm	kp (%)	Dielectric constant	d ₃₁ (10 ⁻¹² C/N)	Loss tangent	Np (Hz·m)
SPS1000	5.98	0.7	62	16.8	5444	66	0.02	2753
SPS1100	6.00	1.3	44	17.5	5491	73	0.024	2653
SPS1200	5.95	2.5	51	16.2	3406	51	0.039	2743
Normal1300	5.87	3.6	169	14	3356	44	0.014	2796
Normal1400	5.78	26	936	38.7	2333	99	0.0068	2942
two-step1300	5.15	1.2	216	8.9	3850	39	0.015	2408
two-step1350	5.55	3.1	243	17.1	3360	56	0.013	2806
two-step1400	5.82	7.5	530	38	2236	87	0.0075	2978

Table 2. Piezoelectric properties of the BaTiO₃ ceramics.

internal stress in the SPS-BT samples. By considering the distorted X-ray diffraction peaks and decrease in transition temperature, it is speculated that the high internal stress still remains in the SPS-BT ceramics even after 12 h postannealing. Regardless of the fabrication methods, the k_p of the fine-grained BT ceramics is low generally. This is probably due to the insufficient poling treatment of the fine-grained samples.

4. Conclusion

By application of SPS, dense Ba(Zr,Ti)O₃ and BaTiO₃ ceramics with fine grains can be obtained. The properties are quite unique, which cannot be easily obtained by other methods. And this method offers applicability to other dielectric and piezoelectric materials and may yields unique properties similar with the ones observed in BaTiO₃ based ceramics.

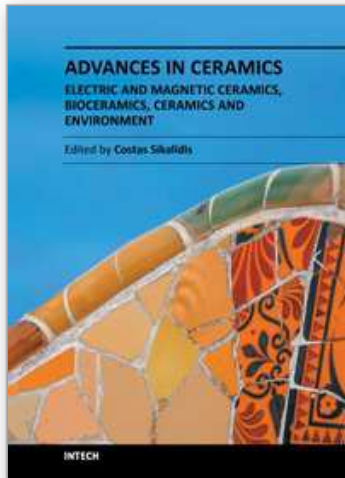
5. Acknowledgment

I would like to thank Mr. Masakazu Kawahara of SPS Syntex Inc. for the spark plasma sintering of the BZT and BT powders. This study was supported in part by a grant-in-aid from the ministry of education (No. 22560671), sports, culture, and technology, Japan and the Iketani science and technology foundation. Some figures and some parts of the sentences are used under the permission of the Japanese Journal of Applied Physics.

6. References

- Arlt, G.; Hennings, D. & De With, G. (1985) Dielectric properties of fine-grained barium titanate ceramics, *Journal of Applied Physics*, Vol. 58, No. 4 (1985) pp. 1619-1925, ISSN 00218979
- Hennings, D.; Schnell, A. & Simon, G. (1982) Diffuse ferroelectric phase transitions in Ba(Ti_{1-y}Zr_y)O₃ ceramics. *Journal of the American Ceramic Society* Vol. 65, No. 11, (November 1982) pp. 539-544, ISSN 0002-7820
- Hungria, T.; Galy, J. & Castro, A. (2009) Spark plasma sintering as a useful technique to the nanostructuration of piezo-ferroelectric materials, *Advanced Engineering Materials*, Vol. 11, No. 8, (August 2009) pp. 615-631, ISSN14381695
- Takegawa, K. et al., (2004) Sintering of lead titanate using a spark-plasma-sintering technique, *Journal of the American Ceramic Society* Vol. 87, No. 4, (April 2004) pp. 541-545, ISSN 0002782
- Karaki, T. et al., (2007). Lead-free piezoelectric ceramics with large dielectric and piezoelectric constants manufactured from BaTiO₃ nano-powder. *Japanese Journal of Applied Physics*, Vol.46, No. 4-7 (February 2007), pp.L97-L98, ISSN 00214922
- Kinoshita, K. & Yamaji, A. (1976) Grain-size effects on dielectric properties in barium titanate ceramics. *Journal of Applied Physics*, Vol. 47, No.1 (1976), pp. 371-373, ISSN 00218979.
- Lines, M. E. & Glass, A. M. (1977) *Principle and Applications of Ferroelectrics and Related Materials*. (Oxford University Press, Oxford, U.K., 1977) p. 532.
- Maiwa, H. (2007) Dielectric and electromechanical properties of Ba(Zr_xTi_{1-x})O₃ (x = 0.1 and 0.2) ceramics prepared by spark plasma sintering *Japanese Journal of Applied Physics*, Vol.46, No. 10b (October 2007), pp. 7013-7017, ISSN 00214922

- Maiwa, H. (2008a) Preparation and properties of BaTiO₃ ceramics by spark plasma sintering *Japanese Journal of Applied Physics*, Vol.47, No.9-2 (September 2008), pp. 7646-7649, ISSN 00214922
- Maiwa, H. (2008b) Structure and properties of Ba(Zr_{0.2}Ti_{0.8})O₃ ceramics prepared by spark plasma sintering *Journal of Materials Sciences*, Vol.43, No. 19 (October 2008), pp. 6385-6390, ISSN 00222461
- Maiwa, H. (2009) Electromechanical properties of BaTiO₃ ceramics prepared by spark plasma sintering and other methods. *Japanese Journal of Applied Physics*, Vol.48, No. 9-2 (2009), pp. 09KD041-09KD044, ISSN 00214922
- Maiwa, H.; Ohashi, K. & Hayashi, T. (2010). Temperature dependence of the electrical and electromechanical properties of Ba(Zr_{0.2}Ti_{0.8})O₃ thin films prepared by chemical solution deposition, *Journal of the Ceramic Society of Japan*, Vol. 118, Issue 1380, (August 2010), pp. 735-737, ISSN 18820743
- Munir, Z. A.; Anselmi-Tamburini, U. & Ohyanagi, M. (2006) The effect of electric field and pressure on the synthesis and consolidation of materials: A review of the spark plasma sintering method, *Journal of Materials Science* Vol. 41, No. 3, (February 2006), pp. 763-777, ISBN 00222461
- Munir, Z. A.; Quach, D. V. & Ohyanagi, M. (2011) Electric current activation of sintering: A review of the pulsed electric current sintering process, *Journal of the American Ceramic Society*, Vol. 94, No.1, (January 2011), pp. 1-19, ISBN 0027820
- Neirman, S. M. (1988). The Curie point temperature of Ba(Zr_{1-x}Zr_x)O₃ solid solutions, *Journal of Materials Science*, Vol. 23, No. 11 (November 1988), pp. 3973-3980, ISBN 00222461
- Takahashi, H. et al., (2006). Piezoelectric properties of BaTiO₃ ceramics with high performance fabricated by microwave sintering. *Japanese Journal of Applied Physics*, Vol. 45, No. 9B (September 2006), pp. 7405-7408, ISSN 00214922
- Takahashi, H. et al., (2008). Considerations for BaTiO₃ ceramics with high piezoelectric properties fabricated by microwave sintering method. *Japanese Journal of Applied Physics*, Vol.47, Issue 11, (November 2008), pp. 8468-8471, ISSN 00214922
- Takeuchi, T. et al., (1999) Preparation of dense BaTiO₃ ceramics with submicrometer grains by spark plasma sintering, *Journal of the American Ceramic Society*, Vol. 82, No. 4, (1999), pp. 939-943, ISSN 00027820
- Wada, T. (2003) Ferroelectric NaNbO₃ ceramics fabricated by spark plasma sintering, *Japanese Journal of Applied Physics*, Vol. 42, No. 9B, (September 2003), pp. 6110-6114, ISSN 00214922
- Xu, J.; Shaikh, A. S. & Vest, R. W. (1989). High K BaTiO₃ films from metalloorganic precursors. *IEEE Transactions on Ultrasonics, Ferroelectrics, and Frequency Control*, Vol. 36, No. 3, (May 1989), pp. 307-312, ISSN 08853010.
- Yu, Z. et al., (2002) Piezoelectric and strain behavior of Ba(Zr_{1-x}Zr_x)O₃ ceramics, *Journal of Applied Physics*, Vol. 92, (August 2002) pp. 1489-1493, ISSN 00218979
- Zhang, B. P. (2006) Compositional dependence of piezoelectric properties in Na_xK_{1-x}NbO₃ lead-free ceramics prepared by spark plasma sintering, *Journal of the American Ceramic Society*, Vol. 89, No. 5, (May 2006) pp. 1605-1609, ISSN 00027820



**Advances in Ceramics - Electric and Magnetic Ceramics,
Bioceramics, Ceramics and Environment**

Edited by Prof. Costas Sikalidis

ISBN 978-953-307-350-7

Hard cover, 550 pages

Publisher InTech

Published online 06, September, 2011

Published in print edition September, 2011

The current book consists of twenty-four chapters divided into three sections. Section I includes fourteen chapters in electric and magnetic ceramics which deal with modern specific research on dielectrics and their applications, on nanodielectrics, on piezoceramics, on glass ceramics with para-, anti- or ferro-electric active phases, of varistors ceramics and magnetic ceramics. Section II includes seven chapters in bioceramics which include review information and research results/data on biocompatibility, on medical applications of alumina, zirconia, silicon nitride, ZrO₂, bioglass, apatite-wollastonite glass ceramic and b-tri-calcium phosphate. Section III includes three chapters in applications of ceramics in environmental improvement and protection, in water cleaning, in metal bearing wastes stabilization and in utilization of wastes from ceramic industry in concrete and concrete products.

How to reference

In order to correctly reference this scholarly work, feel free to copy and paste the following:

Hiroshi Maiwa (2011). Preparation and Properties of BaTiO₃ and Ba(Zr,Ti)O₃ Ceramics by Spark Plasma Sintering, *Advances in Ceramics - Electric and Magnetic Ceramics, Bioceramics, Ceramics and Environment*, Prof. Costas Sikalidis (Ed.), ISBN: 978-953-307-350-7, InTech, Available from:

<http://www.intechopen.com/books/advances-in-ceramics-electric-and-magnetic-ceramics-bioceramics-ceramics-and-environment/preparation-and-properties-of-batio3-and-ba-zr-ti-o3-ceramics-by-spark-plasma-sintering>

INTECH
open science | open minds

InTech Europe

University Campus STeP Ri
Slavka Krautzeka 83/A
51000 Rijeka, Croatia
Phone: +385 (51) 770 447
Fax: +385 (51) 686 166
www.intechopen.com

InTech China

Unit 405, Office Block, Hotel Equatorial Shanghai
No.65, Yan An Road (West), Shanghai, 200040, China
中国上海市延安西路65号上海国际贵都大饭店办公楼405单元
Phone: +86-21-62489820
Fax: +86-21-62489821

© 2011 The Author(s). Licensee IntechOpen. This chapter is distributed under the terms of the [Creative Commons Attribution-NonCommercial-ShareAlike-3.0 License](https://creativecommons.org/licenses/by-nc-sa/3.0/), which permits use, distribution and reproduction for non-commercial purposes, provided the original is properly cited and derivative works building on this content are distributed under the same license.

IntechOpen

IntechOpen